CONF-820274--2

POSITRON-ANNIHILATION SPECTROSCOPY OF VACANCY DEFECTS IN ALUMINUM*

B. Chakraborty†, S. Berko‡, M. J. Fluss‡†, K. Hoffmann‡ P. Lippel‡, and K. W. Siegel†

†Materials Science Division, Argonne National Laboratory
Argonne, Illinois 60439, USA

‡Department of Physics, Brandeis University
Waltham, Massachusetts 02254, USA

CONF-820274--2

DE83 007628

JUNE 1982

*This work was supported by the U.S. Department of Energy (Contract No. W-31-109-ENG-38) and National Science Foundation (Grant DMR-7926035).

To be published in Positron Annihilation Spectroscopy, the Proceedings of the Second National Symposium on Positron Annihilation, Madras, India, 8-12 February 1982.

POSITRON-ANNIHILATION SPECTROSCOPY OF VACANCY DEFECTS IN ALUMINUM*

B. Chakraborty†, S. Berko‡, M. J. Fluss‡†, K. Hoffmann‡ P. Lippel‡, and R. W. Siegel†

†Materials Science Division, Argonne National Laboratory
Argonne, Illinois 60439, USA

‡Department of Physics, Brandeis University
Waltham, Massachusetts 02254, USA

ABSTRACT

Positron annihilation characteristics in a monovacancy and a divacancy in aluminum have been calculated self-consistently using a local density functional formalism, into which the many-body enhancement effects have been incorporated. Results for the theoretical two-dimensional angular correlation of annihilation radiation spectra are compared to experimental results obtained from an aluminum single crystal at 20°C, where positrons annihilate from a Bloch-state, and at higher temperatures, 500°C and 630°C, where they annihilate primarily from vacancy-trapped states.

---

*This work was supported by the U.S. Department of Energy (Contract No. W-31-109-ENG-38) and National Science Foundation (Grant DMR-7926035).

1. INTRODUCTION

Positron annihilation spectroscopy (PAS), can be a very sensitive probe of the electronic structure of vacancy-like defects because of positron trapping at these defects. However, the positron significantly perturbs its electronic environment, making it difficult to deduce the unperturbed defect electronic structure from PAS measurements. Theoretical calculations of positron annihilation characteristics in defects, including the electron-positron correlation effects, are thus necessary. These, together with defect electronic structure calculations in the absence of the positron, can complement the experimental efforts to understand the details of defect electronic structure in metals. Such calculations greatly enhance the utility of the positron as a localized probe of vacancy-like defect structures.

In this paper, the results of theoretical calculations of the annihilation characteristics of monovacancy- and divacancy-trapped positrons in Al are presented. These calculations are based on the recently developed formalism for incorporating many-body enhancement effects into band-structure calculations.[1] Application of this formalism to defect-free Al has yielded results[2] in good agreement with experiment.[3,4] The theoretical results for the Bloch-state and the monovacancy- and divacancy-trapped states of the positron are presented and compared to experimental two-dimensional angular correlation of annihilation radiation (2D-ACAR) data for an Al single crystal at 20°C, where the positron annihilates from its Bloch-state, and for higher temperatures, 500°C and 630°C, where positron trapping at vacancy defects dominates. From earlier experimental studies, it is expected that a signficant concentration of divacancies is present in Al in the equilibrium vacancy ensemble at high temperatures.[5] By comparing the theoretical results to the experimentally observed spectra, one expects to be able to understand

the changes in the nature of the vacancy ensemble in Al as a function of temperature and to possibly develop for the first time a "fingerprinting" method for the vacancy-defects present in the ensemble.

II. THEORY

A completely realistic calculation of positron annihilation characteristics in defects has to incorporate the following features: (i) accurate treatment of the host-metal electronic structure, (ii) self-consistency of the electron and positron potentials, allowing for electronic screening of the defect and the positron, and (iii) structural relaxations around the defect in the presence of the trapped positron. The Green's-function[6,7] and supercell[8-11] methods have been used to study the electronic structure of point defects in solids. Both of these approaches can adequately handle the accurate treatment of the host electronic structure. The Green's-function method treats a truly isolated defect and can be superior to the supercell approach in that respect, but the applications to metals have shown that true self-consistency, even in the absence of the positron, is difficult to achieve.[7,12] The supercell approach was therefore chosen for the present work. The electronic structures of a monovacancy[10,11] and divacancy[11] in Al were previously calculated using the self-consistent pseudopotential method, in which the environments of the vacancy defects were simulated by a supercell containing 27 atomic sites. It was seen that the monovacancy potentials were effectively isolated in this supercell, and that the overlap of wavefunctions from neighboring monovacancies is too small to affect the calculated electronic structure.[10,11] In the 27-atom-site supercell containing divacancies, on the other hand, the overlap of wavefunctions from neighboring defects is not insignificant. However, within the context of calculations of positron annihilation characteristics, the results are expected to be independent of

the supercell configuration, since the positron is well localized within the vacancy defects, and even more so in the divacancy than in the monovacancy, owing to its more deeply bound state.

In order to calculate positron annihilation characteristics, a generalized self-consistent scheme is needed. Such a formalism, based on a two-component density functional scheme, has been developed recently.[1] It is a perfectly general formalism, applicable to any metal, which can be used with any band-structure scheme. A self-consistent pseudopotential band-structure scheme with a plane-wave basis set, which incorporates this formalism, was applied to defect-free Al.[1,2] A norm-conserving, ab initio pseudopotential[13] was used for the electrons and a generalization of the pseudopotential scheme of Kubica and Stott[14] was used for the positron. This scheme yields a calculated positron lifetime and 2D-ACAR Bloch-state spectrum in good agreement with experimental lifetime[4] and 2D-ACAR data.[3] The present calculations of the annihilation characteristics of the defect-trapped states were carried out using this generalized pseudopotential scheme.

III. RESULTS AND DISCUSSION

The calculated positron densities in the monovacancy and the divacancy in Al are shown in Fig. 1. The positron is seen to be quite well localized in both defects. The portion leaking out into the interstitial regions is small, but significant, and is seen to have an anisotropic distribution. Owing to crystal symmetry, a six-fold spatial averaging had to be performed for the divacancy results before comparing with experiment. The positron density in the divacancy after this six-fold averaging is also shown in Fig. 1 and, as expected, exhibits much less anisotropy; the shape of the positron density distribution is now more similar to that in the monovacancy-trapped state. The anisotropy of the monovacancy-trapped state positron distribution is quite

similar to that obtained by Gupta and Siegel.[9] This is the first time that the divacancy-trapped state distribution has been calculated within a crystal lattice; previous jellium calculations have been made.[15,16] The high-momentum components of the 2D-ACAR spectra from the vacancy-trapped states of the positron are expected to reflect the spatial anisotropy of the positron distribution caused by the atoms. The calculated binding energies for the positron to the monovacancy and the divacancy are 2.2 eV and 3.0 eV, respectively. It should be noted that all of these calculations are carried out for a lattice parameter of 4.047 Å, corresponding to that at 0°K in Al.

The present value for the positron binding energy to the monovacancy is roughly similar to those obtained from previous self-consistent jellium calculations,[15,16] but less than the value of 3.4 eV obtained from the non-self-consistent augmented plane wave calculation of Gupta and Siegel.[9] A recent jellium calculation of the binding energy to the divacancy[16] gave a value of 3.2 eV for a spherical model and 2.6 eV for an ellipsoidal model of the divacancy. The positron lifetimes were calculated using the present formalism to be 228 ps in the monovacancy and 255 ps in the divacancy. The experimental value[4] for the monovacancy-trapped positron lifetime at 400°C is 240 ps. The present lifetime values are similar to the results obtained from other theoretical calculations.[9,15,16] The binding energies are seen to be more sensitive than the lifetimes to the proper incorporation of correlation effects.[3]

The 2D-ACAR spectra for these defect-trapped states of the positron have not been previously calculated. The present theoretical 2D-ACAR results for the Bloch-state (N_B), and the monovacancy-trapped (N_{1V}) and divacancy-trapped (N_{2V}) positron states are shown in Fig. 2. The integration direction and the p_y and the p_z axes lie along <100> directions. These calculations are all

normalized to the same volume. Experimental 2D-ACAR data, obtained[17] at Brandeis University using the multicounter cross-correlation 2D-ACAR instrument,[18] are shown in Fig. 3 for 20°C, 500°C, and 630°C (N_{20}, N_{500}, and N_{630}, respectively). The measurements were made on an oriented Al single-crystal sample using circular collimators 1.5 mrad in diameter. The data at temperature T, $N_T(p_y,p_z)$, were obtained with a <100> axis of the crystal oriented along the integration direction p_x and <110> axes along p_y and p_z. The theoretical and experimental spectra in Fig. 2 are rotated with respect to one another accordingly. Also, the experimental resolution function has been incorporated into the theoretical 2D-ACAR results shown in Fig. 2. The peak of $N_B(p_y,p_z)$ has been normalized to the peak of $N_{20}(p_y,p_z)$; volume normalization would have been inappropriate, since the high-momentum components of the Bloch-state spectra are underestimated in the present calculations, owing to the neglect of core-orthogonalization effects.[1,2]

The shape of the Bloch-state spectrum in Fig. 2 can be seen to agree quite well with the experimental 20°C spectrum (Fig. 3), where the positron is expected to annihilate from a free state.[19] At 500°C and 630°C, approximately 94% and 99% of the positrons, respectively, annihilate from vacancy-trapped states according to a two-state trapping model analysis of complementary long-slit data.[17] The experimental spectra at these temperatures, therefore, exhibit primarily the characteristics of the trapped-state annihilation. On comparing the experimental results to the theoretical predictions for the 2D-ACAR surfaces from the two types of vacancy defects considered here, it is seen that N_{500} and N_{630} lie in between N_{1V} and N_{2V} in both shape and magnitude. To make a more detailed comparison, experimental trapped-state spectra (N'_{500}, N'_{630}) were extracted from N_{500} and N_{630} by subtracting the appropriate percentages of N_{20} (6% and 1%, respectively) and renormalizing the

resulting spectra to the original volume. (The additional minor corrections to the Bloch-state spectra in going from 20°C to either 500°C or 630°C were not made). The change in going from the 20°C free-positron state to the 500°C and 630°C trapped states could then be studied by comparing the relative difference spectra, $(N'_{500}-N_{20})/N_{20}(p_y=0,\ p_z=0)$ and $(N'_{630}-N_{20})/N_{20}(0,0)$, to the theoretical relative difference spectra for the two trapped states, $(N_{2V}-N_B)/N_B(0,0)$ and $(N_{2V}-N_B)/N_B(0,0)$. The radial slices along the <110> directions of the various spectra, N_B, N_{1V}, N_{2V} and N_{20}, N'_{500}, N'_{630}, are presented in Figs. 4a and 4b, respectively. It has been deduced from these data[17] that the effect of positron trapping at monovacancies can account for ~90% of the change in peak height in going from 20°C to 500°C, and for ~80% of the change in going from 20°C to 630°C. The general features of the theoretical and experimental spectra are seen to agree quite well, given the fact that the theoretical spectra are all calculated at 0°K (i.e., using the calculated lattice constant of Al at 0°K). This comparison between theory and experiment would be consistent with an increasing population of divacancies[5] from 500°C to 630°C. However, a precise quantitative comparison must await further work on a number of temperature-dependent effects.[17]

Structural (atomic) relaxations around the vacancy defects in the presence of the positron have not been dealt with in any detail in the present work, but they could play an important rôle in changing the 2D-ACAR spectra of the trapped positron states. An analysis of the observed anisotropies in the high-momentum components of the theoretical and experimental 2D-ACAR results in terms of the spatial anisotropies of the positron density (Fig. 1) could prove to be useful in this context. Contour plots of the theoretically calculated spectra, N_{1V} and N_{2V}, and the experimentally determined trapped-state spectra, N'_{500} and N'_{630}, are shown in Fig. 5. The structure at high

momenta in N_{1V} and N_{2V} could be reflecting the anisotropy of the positron density near the atomic sites. The experimentally observed spectra N'_{500} and N'_{630} show a smaller anisotropy than either N_{1V} or N_{2V}. A preliminary estimate[10,11] of the force exerted by the monovacancy-trapped positron on the surrounding atoms, using the Hellmann-Feynman method, indicates that there would be an effective outward pressure on the first-nearest-neighbor atoms around the monovacancy, as previously suggested.[20] This would give rise to a smaller anisotropy in the high-momentum regions of the resulting 2D-ACAR data. Thus, it is plausible that lattice relaxations could explain the observed anisotropies at high temperatures. No definite conclusions can be reached, however, before examining the effect of the relaxations on the 2D-ACAR spectra in more detail. The relaxations around the divacancy have also to be considered. Work is now in progress along these directions.

Thermal effects have been completely left out of the theory until now. Static lattice expansion effects on all three positron states can be examined within the context of the zero-temperature formalism. The effect of static lattice expansion on the monovacancy state from 0°K to 500°C has been calculated. If we assume that the differential change with temperature remains constant throughout the temperature regime, then the additional effect from static expansion of the monovacancy in going from 500°C to 630°C is ~20 times too small to explain the observed experimental changes.[17] At present the 2D-ACAR spectra are being calculated at the experimental lattice constants for the Bloch state and monovacancy- and divacancy-trapped states of the positron. Phonon effects on the Bloch state, effects of local atomic vibrations around the defects, and positron thermal-smearing effects have yet to be examined.

In conclusion, it is clear that the high-temperature 2D-ACAR data exhibit several interesting features that bear further investigation. The small high-momentum anisotropies, which may be associated with the atomic structure of the vacancy defects, should be further investigated. The temperature dependence of the data between 500°C and 630°C should be explainable in terms of the temperature dependence of the equilibrium vacancy ensemble. However, the inclusion of a number of temperature-dependent effects (e.g., the static expansion of the monovacancies and divacancies) into the theoretical calculations must be accomplished. It is already evident, however, that realistic theoretical calculations can complement the experimental efforts in using the 2D-ACAR positron annihilation technique to yield valuable information about the equilibrium vacancy ensemble in metals and the positron response to such defect systems.

REFERENCES

1. B. Chakraborty, Phys. Rev. B 24, 7423 (1981).
2. B. Chakraborty, Proc. Sixth Intl. Conf. on Positron Annihilation, Fort Worth 1982, P. G. Coleman et al., eds., (North-Holland, Amsterdam, 1982); these Proceedings.
3. J. Mader, S. Berko, H. Krakauer, and A. Bansil, Phys. Rev. Lett. 37, 1232 (1976).
4. M. J. Fluss, L. C. Smedskjaer, M. K. Chason, D. G. Legnini, and R. W. Siegel, Phys. Rev. B 17, 3444 (1978).
5. R. W. Siegel, J. Nucl. Mater. 69 & 70, 117 (1978).
6. G. A. Baraff and M. Schlüter, Phys. Rev. B 19, 4965 (1979).
7. R. Zeller and P. H. Dederichs, Phys. Rev. Lett. 42, 1713 (1979).
8. S. G. Louie, M. Schlüter, J. R. Chelikowsky, and M. L. Cohen, Phys. Rev. B 13, 1654 (1976).
9. R. P. Gupta and R. W. Siegel, Phys. Rev. B 22, 4572 (1980).
10. B. Chakraborty, R. W. Siegel, and W. E. Pickett, Phys. Rev. B 24, 5445 (1981).
11. B. Chakraborty and R. W. Siegel, Proc. Yamada Conf. V on Point Defects and Defect Interactions in Metals, Kyoto, 1981, J. Takamura et al., eds., (University of Tokyo Press, 1982) in press.
12. R. Zeller, P. J. Braspenning, J. Dentz, R. Podloucky, and P. H. Dederichs, Proc. Yamada Conf. V on Point Defects and Defect Interactions in Metals, Kyoto, 1981, J. Takamura et al., eds., (University of Tokyo, Tokyo, 1982) in press.
13. D. R. Hamann, M. Schlüter, and C. Chiang, Phys. Rev. Lett. 43, 1494 (1979).

14. P. Kubica and M. J. Stott, J. Phys. F: Metal Phys. 4, 1969 (1974).

15. R. M. Nieminen and M. J. Manninen, in Positrons in Solids, P. Hautojärvi, ed., (Springer, Berlin, 1981) p. 145.

16. T. McMullen, R. J. Douglas, N. Etherington, B. T. A. McKee, A. T. Stewart, and A. Zaremba, J. Phys. F: Metal Phys. 11, 1435 (1981).

17. M. J. Fluss, S. Berko, B. Chakraborty, K. Hoffmann, P. W. Lippel, and R. W. Siegel, Proc. Sixth Intl. Conf. on Positron Annihilation, Fort Worth 1982, P. G. Coleman et al., eds., (North-Holland, Amsterdam, 1982) in press.

18. S. Berko, M. Haghgooie, and J. J. Mader, Phys. Lett. 63A, 335 (1977).

19. There is a small discrepancy between theory and experiment (cf. Fig. 4) arising from a combination of the 0.4 mrad grid size used in the calculation and the required linear interpolation between these points to fold in the resolution function. A <100> slice calculated on a 0.1 mrad grid, showed much better agreement with experiment. However, it is prohibitively expensive to calculate the full 2D-ACAR spectrum on such a fine grid.

20. S. W. Tam and R. W. Siegel, J. Phys. F: Metal Phys. 7, 877 (1977).

FIGURE CAPTIONS

Fig. 1. *Positron density around vacancy defects in the (100) plane; (a)* monovacancy, (b) divacancy, (c) six-fold spatially-averaged *divacancy. The atomic positions are indicated by +.*

Fig. 2. Perspective representations of the calculated 2D-ACAR spectra at 0°K, convoluted with the experiental resolution; (a) Bloch-state, (b) monovacancy- and (c) divacancy-trapped states of the positron. The axes p_z and p_y correspond to <100> directions.

Fig. 3. Perspective representations of the experimental 2D-ACAR data for an Al single crystal at (a) 20°C, (b) 500°C, and (c) 630°C; the axes p_z and p_y correspond to <110> directions.

Fig. 4. Radial slices along <110> of the various 2D-ACAR spectra; (a) N_B, N_{1V}, and N_{2V}, (b) N'_{630}, N'_{500}, and N_{20}. The experimental spectra (b) have been symmetrized.

Fig. 5. Contour plots in the (001) plane of the trapped-state 2D-ACAR spectra, showing anisotropy at high momenta; (a) N_{1V}, (b) N'_{500}, (c) N'_{630}, (d) N_{2V}. The peak heights corresponding to (a), (b), (c) and (d) are 0.4240, 0.4386, 0.4497, 0.4549, respectively. The contour intervals at low momenta (solid lines) and high-momenta (dashed lines) are 0.01 and 0.001, respectively. The axes p_z and p_y correspond to <110> directions. The theoretical plots have been rotated to coincide with the experimental orientation.

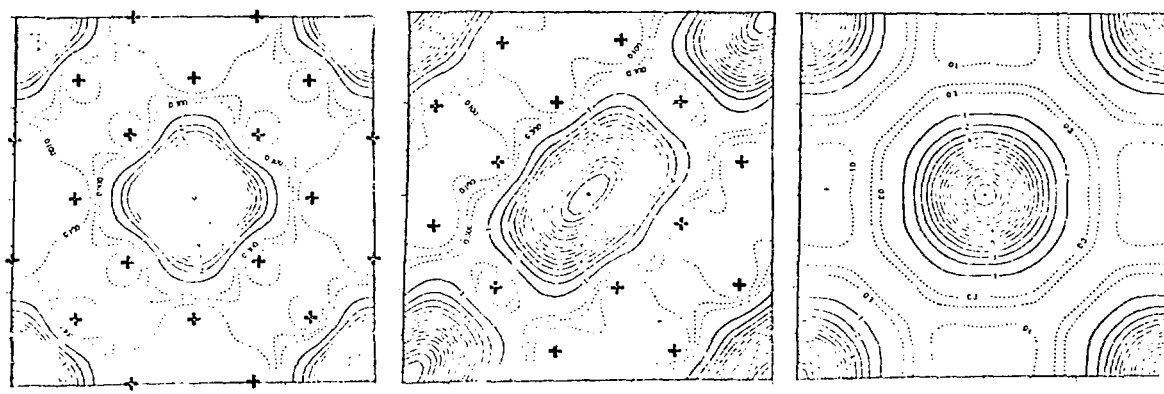

Fig. 1. Positron density around vacancy defects in the (100) plane; (a) monovacancy, (b) divacancy, (c) six-fold spatially-averaged divacancy. The atomic positions are indicated by +.

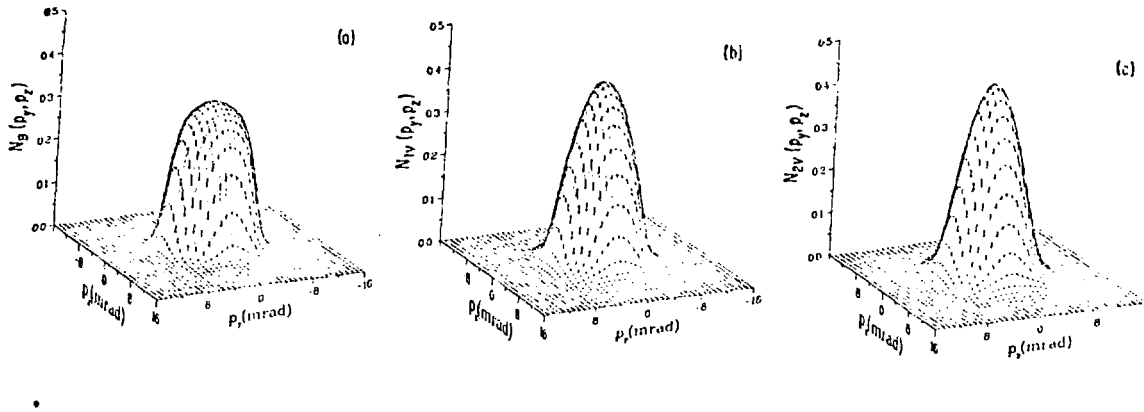

Fig. 2. Perspective representations of the calculated 2D-ACAR spectra at 0°K, convoluted with the experiental resolution; (a) Bloch-state, (b) monovacancy- and (c) divacancy-trapped states of the positron. The axes p_z and p_y correspond to <100> directions.

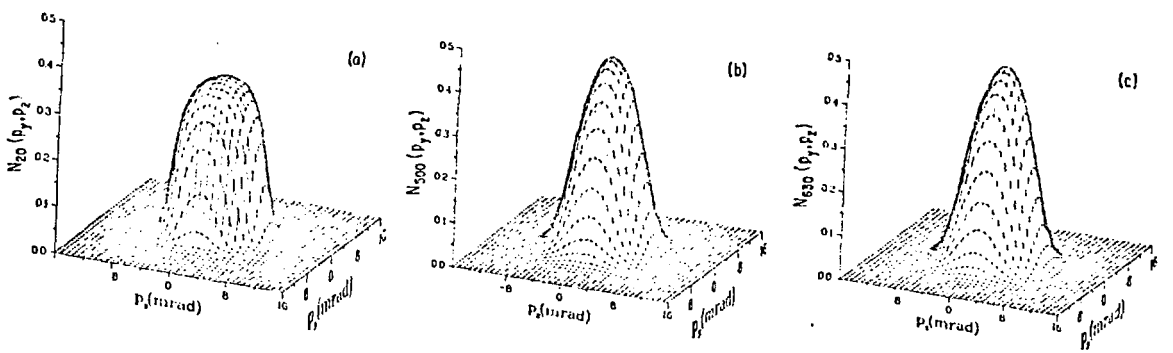

Fig. 3. Perspective representations of the experimental 2D-ACAR data for an Al single crystal at (a) 20°C, (b) 500°C, and (c) 630°C; the axes p_z and p_y correspond to <110> directions.

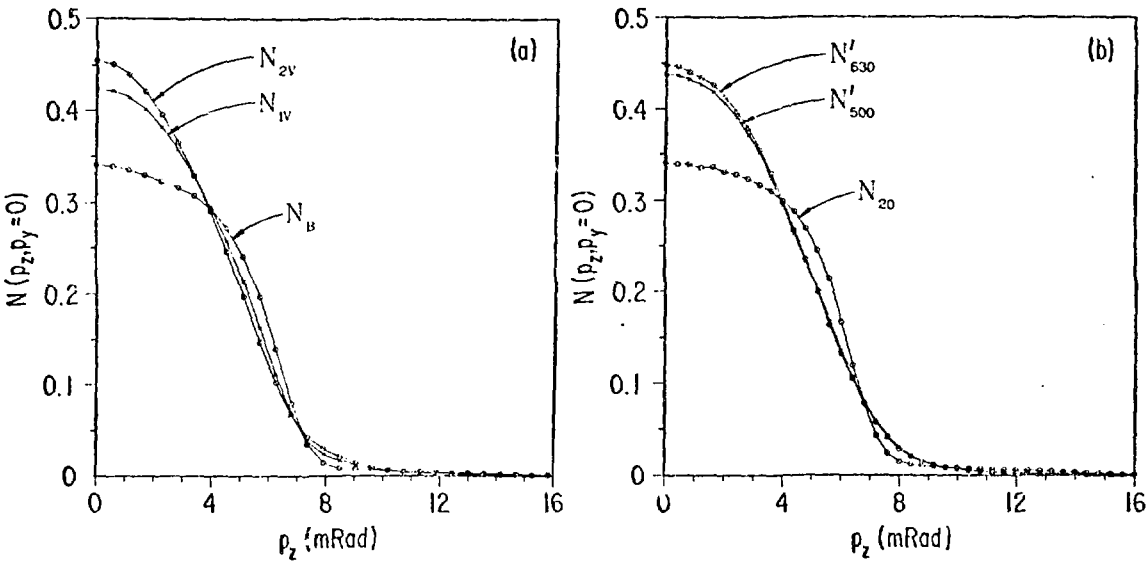

Fig. 4. Radial slices along <110> of the various 2D-ACAR spectra; (a) N_B, N_{1V}, and N_{2V}, (b) N'_{630}, N'_{500}, and N_{20}. The experimental spectra (b) have been symmetrized.

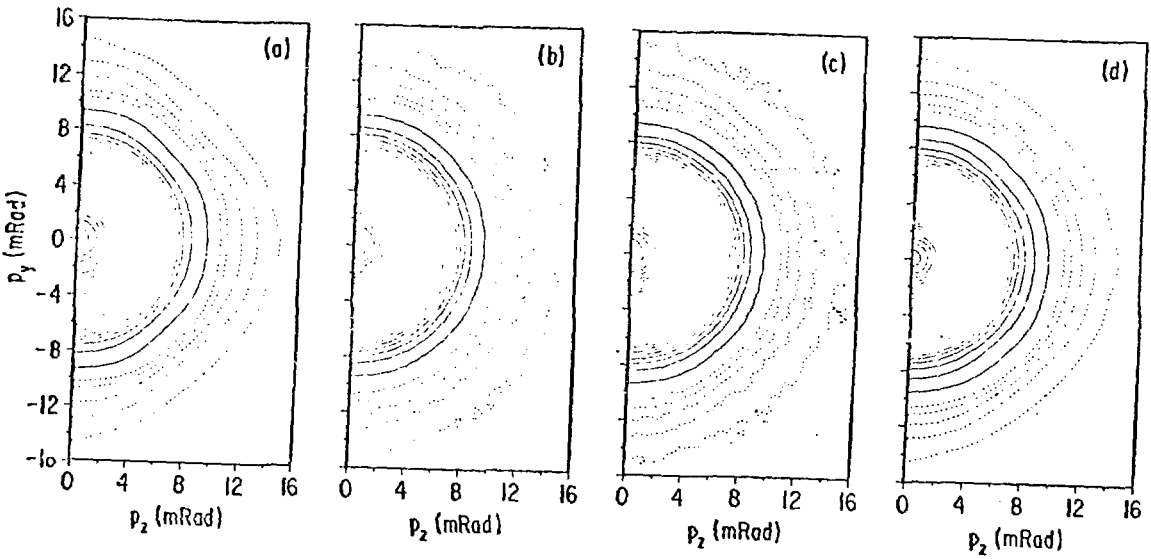

Fig. 5. Contour plots in the (001) plane of the trapped-state 2D-ACAR spectra, showing anisotropy at high momenta; (a) N_{1V}, (b) N'_{500}, (c) N'_{630}, (d) N_{2V}. The peak heights corresponding to (a), (b), (c) and (d) are: 0.4240, 0.4386, 0.4497, 0.4549, respectively. The contour intervals at low momenta (solid lines) and high-momenta (dashed lines) are: 0.01 and 0.001, respectively. The axes p_z and p_y correspond to <110> directions. The theoretical plots have been rotated to coincide with the experimental orientation.